

Abnormal collagen fibrils in tendons of biglycan/fibromodulin-deficient mice lead to gait impairment, ectopic ossification, and osteoarthritis

LAURENT AMEYE,¹ DEAN ARIA, KARL JEPSEN,* AKE OLDBERG,[†] TIANSHUN XU, AND MARIAN F. YOUNG

Craniofacial and Skeletal Diseases Branch, NIDCR, National Institutes of Health, Bethesda, Maryland, USA; *Department of Orthopaedics, Mount Sinai School of Medicine, New York, New York, USA; and [†]Department of Cell and Molecular Biology, University of Lund, Lund, Sweden

ABSTRACT Small leucine-rich proteoglycans (SLRPs) regulate extracellular matrix organization, a process essential in development, tissue repair, and metastasis. In vivo interactions of biglycan and fibromodulin, two SLRPs highly expressed in tendons and bones, were investigated by generating biglycan/fibromodulin double-deficient mice. Here we show that collagen fibrils in tendons from mice deficient in biglycan and/or fibromodulin are structurally and mechanically altered resulting in unstable joints. As a result, the mice develop successively and progressively 1) gait impairment, 2) ectopic tendon ossification, and 3) severe premature osteoarthritis. Forced use of the joints increases ectopic ossification and osteoarthritis in the double-deficient mice, further indicating that structurally weak tendons cause the phenotype. The study shows that mutations in SLRPs may predispose to osteoarthritis and offers a valuable and unique animal model for spontaneous osteoarthritis characterized by early onset and a rapid progression of the disease—Ameys, L., Aria, D., Jepsen, K., Oldberg, A., Xu, T., Young, M. F. Abnormal collagen fibrils in tendons of biglycan/fibromodulin-deficient mice lead to gait impairment, ectopic ossification, and osteoarthritis. *FASEB J.* 16, 673–680 (2002)

Key Words: leucine-rich · proteoglycans · cartilage · bone · matrix

OSTEOARTHRITIS (A HETEROGENEOUS group of conditions characterized by a defective integrity of articular cartilage) is a major cause of disability in humans and one of the most frequent musculoskeletal disorders. More than 80% of individuals over 55 have radiographic evidence of osteoarthritis, 30% of whom will have significant pain or disability, costing billions of dollars in health care annually (1). The existence of genetic risk factors in osteoarthritis is well established, though only a few predisposing genes have been identified (2).

The family of small leucine-rich proteoglycans (SLRPs) currently comprises 11 members. They are characterized by an extracellular localization and a core protein containing a leucine-rich repeat motif (3).

SLRPs are involved in cell metabolism via binding to growth factors and in matrix organization via binding to various collagens (4–8). Three SLRP knockout mice deficient in fibromodulin (*fm*), lumican, or decorin develop abnormal collagen fibrils (7, 9, 10). These collagen abnormalities are associated with corneal opacity in lumican-deficient mice and with skin fragility in decorin-deficient mice (9, 10). Two SLRPs—biglycan (*bgn*) and *fm*—are coexpressed in tendon, cartilage, and bone (11–13). We looked for in vivo interactions between these two proteoglycans by generating *bgn/fm* double-deficient mice.

MATERIALS AND METHODS

Generation of *bgn* and *fm* single and double-deficient mice

All experiments were performed under an institutionally approved protocol for the use of animals in research (#NIDCR-IRP-98–058 and 01–151). Mice deficient in *bgn* or *fm* were generated by gene targeting in embryonic stem cells as described previously (7, 14). Heterozygous *bgn/fm*-deficient mice were produced by breeding a homozygous *bgn*-deficient female (*bgn*^{-/-}/*fm*^{+/+}) with an *fm*-deficient male (*bgn*^{+/0}/*fm*^{-/-}; *bgn* males are designed as *bgn*^{-/0} since the *bgn* gene is located on the X chromosome and absent from the Y chromosome). F2 *bgn/fm* double-deficient (male *bgn*^{-/0}/*fm*^{-/-} and female *bgn*^{-/-}/*fm*^{-/-}) mice were obtained by interbreeding F1 heterozygous *bgn/fm* mice.

Genotyping

All mice were genotyped for *bgn* and *fm* by PCR analysis. The PCR for *bgn* was performed as described by Chen et al. (15). To identify the normal and targeted *fm* alleles, three primers were used: a forward primer corresponding to the 5' end of exon two (5'CCCAGGGCCAGTATGATGAAGACT3'), a reverse primer corresponding to the 3' end of exon two (5'GTTGCGGTTGTACAGTACATGGC5'), and a second reverse primer corresponding to a sequence within the PGK promoter (5'CTTTACGGTATCGCCGCTCCCGATTCCG3')

¹ Correspondence: Nestle Research Center, Dept. Nutrition, G35, Vers-chez-les-Blanc, P.O. Box 44, 1000 Lausanne 26, Switzerland. E-mail: Laurent.Ameys@rdls.nestle.com

of the *fm* targeted allele. PCR parameters for *fm* were the same as for *bgn*, except the PCR buffer contained 2.0 mM MgCl instead of 1.5 mM. PCR products were resolved by electrophoresis through 1.8% agarose gels, yielding bands of 212 bp for wild-type (wt) *bgn* allele, 310 bp for targeted *bgn* allele, 280 bp for wt *fm* allele, and 603 bp for targeted *fm* allele.

Radiographic analysis

Three- and 9-month-old whole animals and their dissected front and hind limbs were analyzed by X-ray with a Faxitron MS-20 specimen radiography system for 90 s at 30 kV using X-OMAT TL Kodak diagnostic films. The semiquantitative scoring systems used to measure the extent of ectopic ossification are described in Fig. 2. The semiquantitative scoring system based on radiographs used to assess the severity of osteoarthritis was the following. A score of 0 corresponded to a healthy joint (joint space well maintained, no evidence of osteophyte formation, no subchondral sclerosis, no cysts), a score of 1 depicted a moderately affected joint (moderate joint space narrowing, presence of osteophytes, no or minimal subchondral sclerosis, no cysts), and a score of 2 corresponded to a severely affected joint (severe narrowing or complete loss of joint space, osteophytes, moderate to severe sclerosis, cysts in some cases).

Histology and electron microscopy analysis

Whole legs were processed for histology as described by Bianco et al. (11). Some legs were processed undecalcified and embedded in methylmethacrylate. Ten micrometer sections were stained with Giemsa and von Kossa. The proximal parts of the quadriceps tendons were processed for transmission electron microscopy as described by Rheinholt et al. (16). The histology-based, semiquantitative scoring system for osteoarthritis consisted of the following. We assigned a score ranging from 0 to 2 for each quadrant of the knee. A score of 0 represented an intact articular cartilage, a score of 1 was given to an articular cartilage surface showing fibrillation and a score of 2 was given to an eroded articular cartilage.

Tread-mill running regimen

Three wt and three *bgn/fm* double-deficient mice were subjected at 1 month of age to daily running on a 1055M-D40 Exer 6M open treadmill (Columbus Instruments, Columbus, OH). Mice ran 6 meters/min for 30 min once a day, 5 days a week. After 1 month, we killed the animals by CO₂ inhalation. As controls, we used three wt and three double-deficient age-matched mice that were not forced to run. We radiographed the legs before processing for histology.

Biomechanical analysis

Tendons stiffness was determined from monotonic failure tests. Flexor digitorum longus (FDL) tendons were loaded by clamping the ends of the tendon between sandpaper-covered plates. They were preconditioned to constant stiffness and energy loss (hysteresis), then loaded to failure at 1%/s. Patella tendons were loaded by clamping the patella and quadriceps tendon between sandpaper-covered plates. The tibia was embedded in epoxy up to the distal insertion site within a brass tube. Patella tendons were loaded to failure at 0.1 mm/s using a custom-built loading device. Mechanical tests were conducted at room temperature using a servohydraulic materials testing system (Instron, Canton, MA). Stiffness was calculated from a linear regression of the load-

deformation curve. Cross-sectional areas of the tendons were determined under transmitted light microscopy, using public domain image analysis software (Scion Corp., Frederick, MD), after fixation of the contralateral limbs in 10% neutral buffered formalin and embedding in poly-methylmethacrylate.

Statistical analysis

The radiographic semiquantitative scores and the fibril diameters were analyzed by one-way ANOVA and Fisher post hoc test. In the running experiment, the scores were compared with a Mann-Whitney test. Biomechanical data were compared using a *t* test with Welch's correction for unequal variances. $P < 0.05$ was considered statistically significant.

RESULTS

Bgn/fm double-deficient mice display gait impairment

The *bgn/fm* double-deficient mice were obtained with the expected Mendelian frequency. Males and females were both fertile. They did not exhibit any gross anatomical abnormalities at any age but were smaller than the wt or either single mutant. At 1, 3, 6, and 9 months, male and female double mutants weighed less than the wt or either single mutant ($P < 0.05$, Fig. 3A). A smaller, generally not statistically significant, weight difference existed between single mutants and wt for both sexes at all times tested (Fig. 3A).

Behavioral observations revealed an abnormal gait characterized by decreased flexibility of knee and ankle joints (i.e., dragging leg) only in double-deficient mice (see Fig. 1A). The dragging was transient and could occur on and off on the right or left side. The abnormal gait was apparent at weaning (3 wk). It persisted until the end of the experiments (9 months), did not appear to progress, and never prevented mice from moving in the cages.

Bgn/fm double-deficient mice develop ectopic tendon ossification subsequent to gait impairment

Radiographs of 3-month-old mice revealed ectopic radio-dense areas in the Achilles tendon and/or in the patellar and quadriceps tendons of the knee in all three populations of mutant mice (Fig. 1B, C). The radio-dense areas in knee and ankle joints were larger and/or more numerous in double mutants than in either single mutant. If these relatively large radio-dense areas were also present in 1-month-old double mutants who already exhibit gait impairment, they could be sufficient to account for abnormal gait. However, radio-dense areas were either undetectable or barely visible. (When scored by the semiquantitative criteria described below, radio-dense areas in these mice always received the smallest scores: 0 or 1.) Thus, the cause of the gait impairment must be something else. With increasing age, other joints (elbow, wrist, and hip) began to

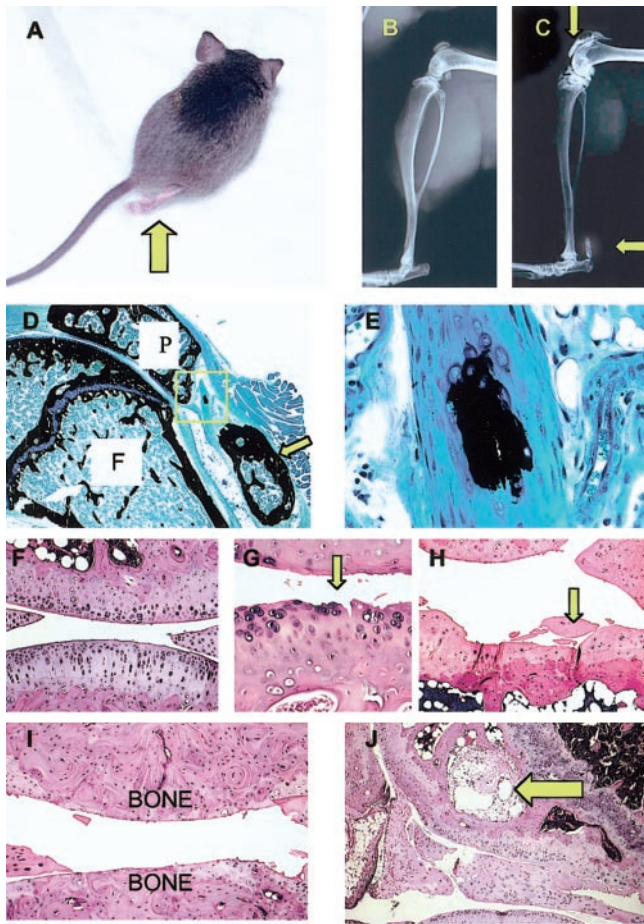


Figure 1. Phenotype of *bgn/fm* double-deficient mice at 1 (A), 3 (D, E, G), 6 (B, C, F, H, I), and 9 months (J). A) Gait impairment characterized by dragging hind limbs while walking (arrow). B–E) Ectopic ossification of tendons. B) X-ray from a WT hind limb. C) X-ray from a double mutant hind limb. The arrows identify radio-dense areas corresponding to ectopic bone formation around the patella and ankle (arrows). D) Von Kossa-stained sagittal section of a hind limb from a double mutant. Note the large ectopic bone (arrow) F; femur. P: patella. E) Enlargement of the boxed area in panel D. Early stage in the development of an ectopic bone within the quadriceps tendon. Mineral is stained black. F) Hematoxylin and eosin-stained sagittal section of a WT mouse knee. Note smooth surfaces of the articular cartilages vs. panels G, H. G–I) Progressive osteoarthritis in the double mutant knees (H&E-stained sagittal sections). G) Fibrillation of articular cartilage (arrow). H) Erosion (detachment) of articular cartilage from the bone (arrow). I) Complete erosion (eburnation) of the articular cartilages in the femur and tibia (upper and lower bones, respectively). J) Cyst (arrow) in the bone marrow cavity of the tibia.

display radio-dense areas in the double mutants but not in either single mutant. Histological examination revealed that the ectopic radio-dense areas in tendons were bones (Fig. 1D). These ectopic bones developed by differentiation of ectopic fibrocartilage, which ossified with age (Fig. 1E). Serum analyses did not detect any significant differences in the levels of bicarbonate, calcium, and phosphorus between wt and any of the mutants (data not shown), indicating that the stimulus

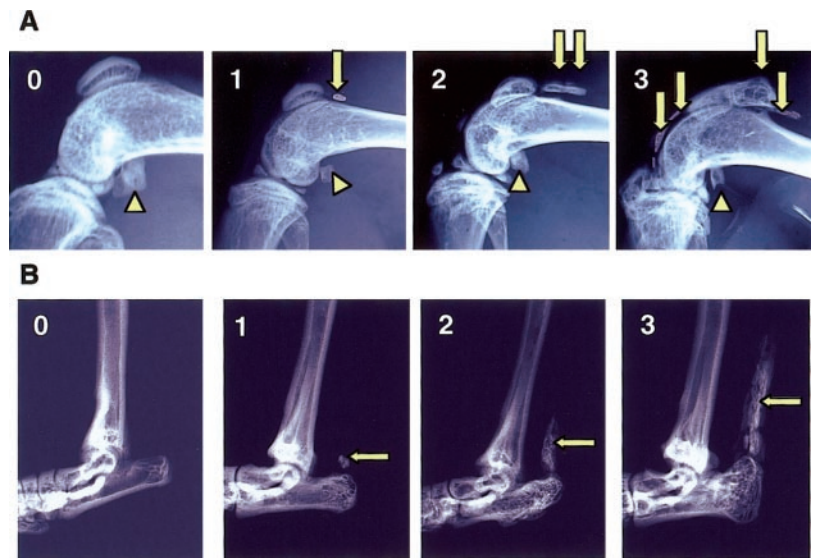
leading to ectopic ossification had a local origin and did not arise from a general metabolic imbalance.

To describe and compare the ectopic ossification revealed on different radiographs, we devised semi-quantitative criteria for classifying the extent of ossification in the knee and ankle into four categories (see Fig. 2A, B). We scored only males because males were affected more than females (data not shown) and so presented greater differences. We calculated the average scores for 3- and 9-month-old animals (Fig. 3B, C). Usually (but not always) the severity of the ossification increased significantly with age, even in the wt, and varied in a genotype-specific manner for the knee and ankle. The absence of *bgn* or *fm* in the single mutants had joint-specific and age-specific effects. For example, in 3-month-old knees, *bgn* deficiency caused significant ectopic ossification that did not significantly increase with age. In contrast, *fm*-deficient knees were not dramatically different from wt knees at either 3 or 9 months. The opposite was true for ankles: *fm* deficiency caused significant ectopic growth in 3-month-old animals that did not become more severe by 9 months, whereas *bgn*-deficient ankles were not significantly different from wt at either age. Since *bgn* and *fm* single deficiencies had different effects on tendon ossification in the knee and ankle, *bgn* and *fm* must have specific expression patterns and/or functions in these tissues. The effect of the double deficiency on ectopic ossification in knees and ankles was dramatic: it was significantly greater and occurred much earlier. That is, the simultaneous absence of *bgn* and *fm* produced a synergistic effect (instead of an expected additive effect) on the extent of ectopic ossification in knees and ankles. This was particularly evident in the ankle at 3 months. Because *bgn*-deficient ankles were not very different from wt, one might have expected the ossification score of the double-deficient ankles to be similar to the score of the *fm*-deficient ankles. Instead, the ossification score of the double-deficient ankles was significantly higher. Observations of such synergistic effects in double mutants suggest that compensatory mechanisms exist in single mutants.

Bgn/fm double-deficient mice develop severe premature osteoarthritis

Histological observations detected osteoarthritis-like lesions in the knee joints of double mutants at 3 months, when the mice already displayed gait impairment and significant ectopic ossification of their patellar, quadriceps, and Achilles tendons. These osteoarthritic lesions, which were never detected at 1 month, led in some cases to a complete erosion of the articular cartilage by 6 months. Both single mutants also developed similar degenerative joint disease, but with a delayed onset. By comparison, surfaces of the tibial and femoral articular cartilage of even the oldest wt animals examined (9 months) were smooth and even (Fig. 1F). The disease progressed as follows. Articular cartilage degeneration first appeared on the tibial plateau and was only

Figure 2. Examples of scoring criteria used to semiquantitate the amount of ectopic ossification in the knee and ankle joints. A score ranging from 0 to 3 was assigned independently to knees (A) and ankles (B) from each animal based on the extent of ectopic radio-dense areas observed on radiographs. A score of 0 indicated the absence of any detectable ectopic radio-dense area. A score of 1 indicated in the knee the presence of one or two small ectopic areas and, in the ankle, a barely visible ectopic area. A score of 2 indicated in the knee three or more small ectopic radio-dense areas or the presence of a single ectopic area with a size similar to the size of the patella and, in the ankle, the occurrence of an easily visible ectopic area. A score of 3 corresponded in the knee and ankle to extensive ectopic radio-dense areas. Arrows point to typical ectopic radio-dense area; arrowheads point to physiological bones of the knee joint.



somewhat delayed on the femoral plateau. Articular cartilages on medial and lateral sides of the joint were affected. The initial degeneration was characterized by one or several clefts in the articular cartilage (fibrillation) (Fig. 1G). Subsequently, pieces of articular cartilage detached and were found in the joint cavity (Fig. 1H). Finally, the entire cartilage layer disappeared, leaving the joint bones unprotected and rubbing directly against each other (eburnation) (Fig. 1I). The subchondral bone became sclerotic under the area of erosion before sclerotic bone filled the whole epiphysis. None of the diseased joints at any time showed evidence of a proliferation reaction or tendency toward regeneration in the articular cartilage. However, osteophytes developed on the tibia and femur surfaces. Although none of the joints showed evidence of inflammation, we observed extensive metaplasia in the meniscus and synovial tissue. In some cases, cysts developed in the marrow of the epiphysis of the head of the tibia (Fig. 1J). In some of the most severely afflicted specimens, condyles of the femur were subluxated dorsal to the head of the tibia. The patella was often displaced and, similar to the disease in humans, clusters of chondrocytes were present in the femoral articular cartilage facing the patella. Under a dissecting microscope, we also noticed early signs of articular cartilage surface degeneration on the medial side of the proximal head of the femur in 9-month-old double mutants.

To compare the mice, we designed a semiquantitative scoring system based on radiographs similar to that used to evaluate osteoarthritis in humans (see Materials and Methods). We calculated average scores for each population of 3- and 9-month-old male mice (Fig. 3D). Although a statistically significant level of osteoarthritis developed by 3 months in the absence of *bgn*, the 3-month-old *fm*-deficient mice were not significantly different from wt. Double mutants were significantly more affected than the wt and single mutants at 3 and 9 months.

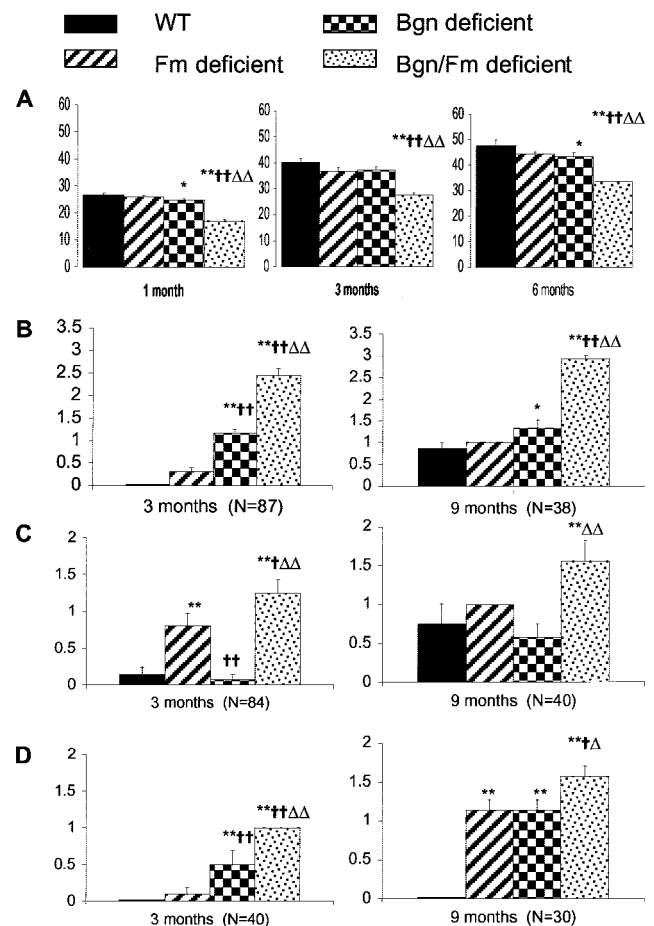


Figure 3. Average weight at 1, 3, and 6 months (A) and average semiquantitative scores for ectopic ossification in knees (B), ankles (C), and for osteoarthritis in knees (D) at 3 and 9 months in wt, *fm*-deficient, *bgn*-deficient, and *bgn/fm* double-deficient mice. * $P < 0.05$ vs. wt, ** $P < 0.01$ vs. wt, † $P < 0.05$ vs. *fm*-deficient mice, †† $P < 0.01$ vs. *fm*-deficient mice, Δ: $P < 0.05$ vs. *bgn*-deficient mice, ΔΔ: $P < 0.01$ vs. *bgn*-deficient mice. The absence of error bars on some columns indicates that all mice/joints had identical scores.

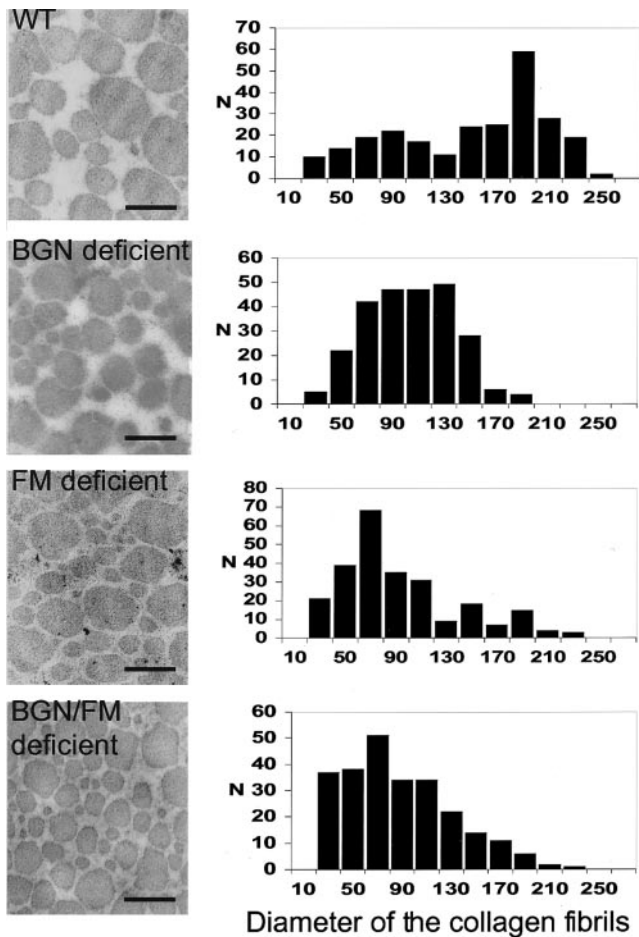


Figure 4. Collagen fibrils in quadriceps tendon at 3 months in wt, bgn-deficient, fm-deficient, and bgn/fm double-deficient mice. Transmission electron microscopic pictures of cross sections of collagen fibrils (left panels) and size distributions of collagen fibril diameters (right panels). Bar 200 nm.

Collagen fibrils in tendons of bgn/fm double-deficient mice are smaller and have abnormal morphology

Because the stimulus leading to tendon ectopic ossification appeared to be local (see above), we decided to perform an electron microscopic analysis of the collagen fibrils in the quadriceps tendon. Compared with wt fibrils, which are rounded, shapes of the collagen fibrils were more irregular in the three mutants (**Fig. 4**). A quantitative analysis of fibril diameters demonstrated statistically significant changes in range, mean, and distribution profiles among the different genotypes (**Fig. 4** and **Table 1**). On average, the fibrils in each mutant were smaller than wt fibrils ($P < 0.05$). The absence of bgn alone resulted in a narrower range of fibril diameters due to the absence of large fibrils (>190 nm) and to a more uniform diameter distribution. In contrast, the absence of fm alone did not affect the fibril diameter range, but resulted in a population dominated by small fibrils (<80 nm). The simultaneous absence of bgn and fm resulted in even more dramatic changes, with an increased number of very

small fibrils (<40 nm). Different from the situation observed in the quadriceps tendon, the collagen fibrils in the articular cartilage of the fm-deficient mice were not different from those observed in the wt cartilage (data not shown). This suggests that, at least in the case of the fm mutant, the osteoarthritis does not result from a collagen defect in the articular cartilage.

Tendons in bgn/fm double-deficient mice are mechanically compromised

To test whether the structural changes observed in the tendons were correlated with altered biomechanical properties, we compared the stiffness of the patellar and FDL tendons in the wt and double mutants at 1 month, before the tendons begin to ossify. Whole tendon stiffness was significantly lower in double mutants relative to the wt for patella (3.38 ± 0.92 N/mm vs. 7.78 ± 1.85 N/mm, $P < 0.001$) and FDL tendons (4.93 ± 1.23 N/mm vs. 10.67 ± 2.11 N/mm, $P < 0.001$). We normalized the stiffness results by the cross-sectional area of each tendon to determine if the differences in tendon stiffness were not simply a scaling artifact due to the smaller size of the double mutants. FDL tendons of the double mutants mice exhibited a 20% smaller stiffness/area ratio than the wt (50.1 ± 15.5 N/mm³ vs. 62.5 ± 15.8 N/mm³, $P < 0.2$) whereas the patella tendons had a 45% smaller stiffness/area ratio (17.3 ± 7.3 N/mm³ vs. 31.6 ± 5.3 N/mm³, $P < 0.006$). These results indicated that tendons from 1-month-old bgn/fm double-deficient mice were less stiff than wt tendons.

Increased use of the joints amplifies tendon ossification and osteoarthritis in double-deficient mice

To gain insight into the processes contributing to this complex phenotype, we devised a simple testable model. We theorized that the reduced stiffness of the bgn/fm-deficient tendons could destabilize the knee joint. This mechanical instability could during joint movement allow abnormal impact and erosion of cartilage. At some time during this destructive phase, the animal responds to the purely mechanical defects by inducing ectopic bone formation. We tested whether the use of the leg joints contributed to the disease progression. If our theory was correct, increased use of the joints should amplify the phenotype of the bgn/fm-deficient mice. We subjected wt and double mutant

TABLE 1. Mean, median, and range of collagen fibril diameters in quadriceps tendons at 3 months

	Wt	Bgn deficient	Fm deficient	Bgn/fm deficient
Mean	150	105*	95* ^Δ	90* ^Δ
Median	166	105	79	80
Range	30–261	35–199	32–245	24–223

* $P < 0.05$ vs. wt, ^Δ $P < 0.05$ vs. bgn-deficient mice.

males to moderate daily running for a month, after which we compared them with mice that were not forced to run. We started the running at 1 month when the articular cartilage was still intact in the mutants. We assessed ectopic ossification with the same scoring system described above (Fig. 2) and assessed osteoarthritis with a semiquantitative scoring system based on histology (see Material and Methods). As predicted, daily running increased ectopic ossification and resulted in more severe osteoarthritis in the double mutants (total scores of 23 and 13 for ectopic ossification in the forced and nonforced runners, respectively, and total scores of 26 and 14 for osteoarthritis in the forced and nonforced runners, respectively; $P < 0.05$ in both cases). In contrast, forced running of wt mice did not increase the scores for either ectopic ossification or osteoarthritis (all total absolute scores equaled to 0).

DISCUSSION

Absence of *bgn* and *fm* in the mouse leads successively and progressively to 1) gait impairment, 2) ectopic tendon ossification, and 3) severe premature osteoarthritis. This first report of ectopic ossification and osteoarthritis in SLRP-deficient mice enlarges the list of defects and affected tissues in these mice. It demonstrates that *bgn* and *fm* are involved, directly or indirectly, in the assembly of normal tendons, in the maintenance of articular cartilage, and in the control of bone growth during aging.

The different components of the phenotype of the mutants can all be explained by a collagen defect in tendons (Fig. 5). The absence of *bgn* and *fm* hinders collagen assembly and results in an excessive number of very small collagen fibrils in tendons that decreases the tendon stiffness. As a result, tendons are unable to hold bones in their normal alignment. This leads to subluxation, and possibly to reversible dislocation of the joints, resulting in decreased joint flexibility and gait impairment. The joint subluxations in turn probably create abnormal mechanical forces within the tendons that may trigger their ectopic ossification. Indeed, the development of fibrocartilage in tendons, the first step in forming sesamoid bones, is known to be a direct response to altered mechanical loading forces (17) whereas the elimination of compressive forces has been shown *in vivo* to result in rapid depletion of fibrocartilage (18). The observation of well-developed sesamoid bones in young double mutants suggests that the absence of *bgn* and *fm* accelerates the transformation of fibrocartilage into sesamoid bone. It would be interesting to determine whether the levels of expression of *bgn* and *fm* are decreased in the patellar tendons of patients affected by the double patella syndrome (19). Mechanically, sesamoid bones help to protect the tendon from damage and in some cases increase the efficiency of the associated muscle (17). Since ossified tendons will have increased stiffness, ossification can be seen as a localized attempt to compensate for the

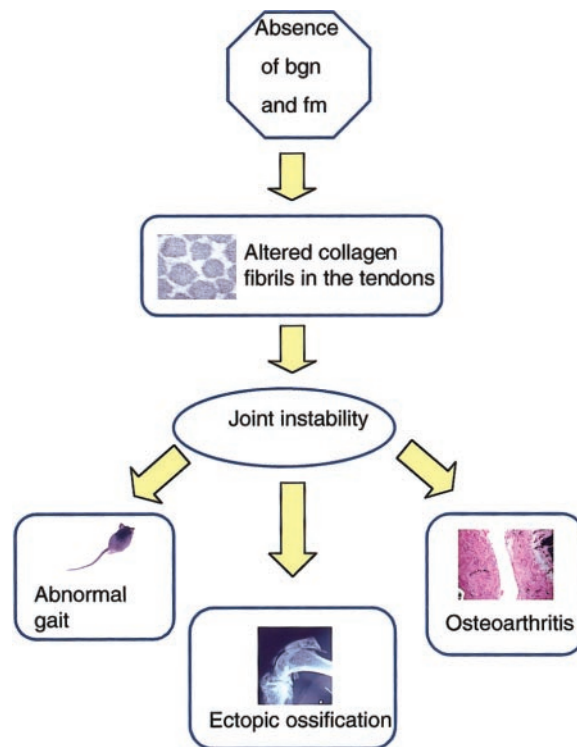


Figure 5. A mechanistic model depicting how the absence of *bgn* and *fm* leads to gait impairment, ectopic ossification of the tendons, and premature osteoarthritis.

original decreased stiffness of the tendons. Besides leading to tendon ossification, joint subluxations result in abnormal contact and impact between the articular cartilage surfaces of the bones. While walking and/or running, the abnormal repetitive impacts between misaligned bones would damage the articular cartilage surfaces and lead to the severe premature osteoarthritis observed. This mechanistic model is supported by the experiment showing that forced joint use increases ectopic ossification and osteoarthritis in the double mutants. In accordance with our observations, osteoarthritis has also been attributed to collagen metabolism abnormalities and mechanical tendon weaknesses in the STR/ORT mouse, another mouse model for spontaneous osteoarthritis (20, 21). However, we cannot exclude the possibility that ectopic ossification and osteoarthritis could result primarily from the involvement of *bgn* and/or *fm* in bone formation. Both proteoglycans bind transforming growth factor β (4) and *bgn* is a positive regulator of bone formation that controls peak bone mass (14).

This simple model in which structurally weak tendons can lead to tendon ossification and osteoarthritis has several interesting and perhaps medical implications. There is strong circumstantial evidence that spontaneous osteoarthritis in humans, like osteoarthritis in *bgn*- and *fm*-deficient mice, is associated with tendon weaknesses and the presence of sesamoid bones. A recent study of 41 patients treated for primary osteoarthritis with no history of ligament injury showed that, at total knee replacement, 20 had missing anterior

cruciate ligaments and another 10 had ligament damage (22). In addition, the high prevalence of osteoarthritis in former soccer players and American football players' knees has been attributed to the high incidence of meniscectomy and cruciate ligament injuries (23). The correlation between obesity and osteoarthritis of the knee (23) could also be explained by the reduced capacity of normal tendons to keep the bones normally aligned in the presence of increased weight. Thus, whether caused by genetic defects, increased weight, or injuries, weakened tendons can lead to premature osteoarthritis and possibly to ectopic tendon ossification. Indeed, the presence of a fabella (a sesamoid bone that sometimes develops in the gastrocnemius tendon of the knee) has been linked to primary osteoarthritis in human knees (24).

Osteoarthritis in *bgn* and *fm* mutants shows a striking similarity to human osteoarthritis. The progressive degeneration of the articular cartilage from early fibrillation to complete erosion, an absence of inflammation, the subchondral sclerosis, and development of osteophytes and cysts are all hallmarks of human osteoarthritis. These similarities suggest that the disease may follow a similar common pathogenetic pathway in both species. Thus, even if the etiology of the disease in these mutants differs from humans, these mice nonetheless constitute valuable models for unraveling the common molecular pathways underlying this disease.

Recent interest in developing treatments for osteoarthritis has become a major focal point in academia and pharmaceutical arenas. Therapy for osteoarthritis has been largely palliative, focusing on alleviation of symptoms. There is therefore a critical need to develop new treatments aimed at slowing down the degenerative process of the disease. Several murine models for osteoarthritis (harboring diverse mutations in collagen types II, IX, and XI) have already been genetically engineered (25–30) and could be used to evaluate new therapeutic agents. However, the *bgn/fm* double-deficient mouse offers three major advantages for this purpose: osteoarthritis starts very early (between 1 and 2 months), its progression is rapid (complete erosion of the articular cartilage between 3 and 6 months), and the disease process can be accelerated by moderate levels of forced treadmill running. Compared with other natural or transgenic models of osteoarthritis, this mouse presents an earlier and faster progression of the disease, making it a model of choice for rapid advances in osteoarthritis research. In parallel or alternatively, a more slowly evolving osteoarthritis with comparable etiology can be investigated in the biglycan or fibromodulin single deficient mouse. The wide variety in rate of progression of osteoarthritis in the SLRP-deficient mice is currently unmatched by any other animal model, making these mice important new tools with which to investigate the molecular mechanisms underlying osteoarthritis. FJ

We thank Linda Browsers and Bill Swaim for help with electron microscopy analysis, Andrew Ayers for help with the

radiographic assessment of osteoarthritis, Georgina Miller for helping with the histological interpretation of the pathology, Albert Kingman for his assistance with the statistical analysis, and Shutki Chakravarti for providing the *fm*-deficient mice. We also thank Larry Fisher, Mike Collins, Arabella Leet, and Xiao-Dong Chen for their advice and generous technical training, and Pamela Gehron Robey and Stan Gronthos for critical reading of the manuscript.

REFERENCES

- Schwartz, S., and Zimmermann, B. (1999) Update on osteoarthritis. *Med. Health* **82**, 321–324
- Vikkula, M., and Olsen, B. R. (1996) Unraveling the molecular genetics of osteoarthritis. *Ann. Med.* **28**, 301–304
- Matsumura, N., Ohyanagi, T., Tanaka, T., and Kretsinger, R. (2000) Super-motifs and evolution of tandem leucine-rich repeats within the small proteoglycans—biglycan, decorin, lumican, fibromodulin, PRELP, keratocan, osteoadherin, epiphycan, and osteoglycin. *Proteins* **38**, 210–225
- Hildebrand, A., Romaris, M., Rasmussen, L., Heinegard, D., Twardzik, D., Borders, W., and Ruoslahti, E. (1994) Interaction of the small interstitial proteoglycans, decorin and fibromodulin with transforming growth factor β . *Biochem. J.* **302**, 527–534
- Hocking, A. M., Shinomura, T., and McQuillan, D. J. (1998) Leucine-rich repeat glycoproteins of the extracellular matrix. *Matrix Biol.* **17**, 1–19
- Iozzo, R. (1999) The biology of the small leucine-rich proteoglycans. *J. Biol. Chem.* **274**, 18843–18846
- Svensson, L., Aszodi, A., Reinholt, F., Fassler, R., Heinegard, D., and Oldberg, A. (1999) Fibromodulin-null mice have abnormal collagen fibrils, tissue organization, and altered lumican deposition in tendon. *J. Biol. Chem.* **274**, 9636–9647
- Ezura, Y., Chakravarti, S., Oldberg, A., Chervoneva, I., and Birk, D. E. (2000) Differential expression of lumican and fibromodulin regulate collagen fibrillogenesis in developing mouse tendons. *J. Cell Biol.* **151**, 779–787
- Chakravarti, S., Magnuson, T., Lass, J., Jepsen, K., LaMantia, C., and Carroll, H. (1998) Lumican regulates collagen fibril assembly: skin fragility and corneal opacity in the absence of lumican. *J. Cell Biol.* **141**, 1277–1286
- Danielson, K., Baribault, H., Holmes, D., Graham, H., Kadler, K., and Iozzo, R. (1997) Targeted disruption of decorin leads to abnormal collagen fibril morphology and skin fragility. *J. Cell Biol.* **136**, 729–749
- Bianco, P., Fisher, L., Young, M., Termine, J., and Gehron Robey, P. (1990) Expression and localization of the two small proteoglycans biglycan and decorin in developing human skeletal and non-skeletal tissues. *J. Histochem. Cytochem.* **38**, 1549–1563
- Saamanen, A.-M., Salminen, H. J., Rantakokko, A. J., Heinegard, D., and Vuorio, E. I. (2001) Murine fibromodulin: cDNA and genomic structure, and age-related expression and distribution in the knee joint. *Biochem. J.* **355**, 577–585
- Wilda, M., Bachner, D., Just, W., Geerkens, C., Kraus, P., Vogel, W., and Hameister, H. (2000) A comparison of the expression pattern of five genes of the family of small leucine-rich proteoglycans during mouse development. *J. Bone Min Res.* **11**, 2187–2196
- Xu, T., Bianco, P., Fisher, L., Longenecker, G., Smith, E., Goldstein, S., Bonadio, J., Boskey, A., Heegaard, A., Sommer, B., Satomura, K., Dominguez, P., Zhao, C., Kulkarni, A., Gehron-Robey, P., and Young, M. (1998) Targeted disruption of the biglycan gene leads to an osteoporosis-like phenotype in mice. *Nat. Genet.* **20**, 78–82
- Chen, X.-D., Shi, S., Xu, T., Gehron-Robey, P., and Young, M. (2002) Age-related osteoporosis in biglycan deficient mice is related to defects in bone marrow stromal cells. *J. Bone Min. Res.* **17**, 331–340
- Reinholt, F. P., Engfeldt, B., Hjerpe, A., and Jansson, K. (1982) Stereological studies on the epiphyseal growth plate with special reference to the distribution of matrix vesicles. *J. Ultrastruct. Res.* **80**, 270–279

17. Sarin, V. K., Erickson, G. M., Giori, N. J., Bergman, A. G., and Carter, D. R. (1999) Coincident development of sesamoid bones and clues to their evolution. *Anat. Rec.* **257**, 174–180
18. Malaviya, P., Butler, D. L., Boivin, G. P., Smith, F. N., Barry, F. P., Murphy, J. M., and Vogel, K. G. (2000) An in vivo model for load-modulated remodeling in the rabbit flexor tendon. *J. Orthop. Res.* **18**, 116–125
19. Cipolla, M., Cerullo, G., Franco, V., Gianni, E., and Puddu, G. (1995) The double patella syndrome. *Knee Surg. Sports Traumatol. Arthroscopy* **3**, 21–25
20. Walton, M. (1977) Degenerative joint disease in the mouse knee; histological observations. *J. Pathol.* **123**, 109–122
21. Anderson-MacKenzie, J. M., Billingham, M. E., and Bailey, A. J. (1999) Collagen remodeling in the anterior cruciate ligament associated with developing spontaneous murine osteoarthritis. *Biochem. Biophys. Res. Commun.* **258**, 763–767
22. Wada, M., Imura, S., Baba, H., and Shimada, S. (1996) Knee laxity in patients with osteoarthritis and rheumatoid arthritis. *Br. J. Rheumatol.* **35**, 560–563
23. Nuki, G. (1999) Osteoarthritis: a problem of joint failure. *Z. Rheumatol.* **58**, 142–147
24. Pritchett, J. W. (1984) The incidence of fabellae in osteoarthrosis of the knee. *J. Bone Joint Surg. Am.* **66**, 1379–1380
25. Fassler, R., Schnegelsberg, P. N., Dausman, J., Shinya, T., Muragaki, Y., McCarthy, M. T., Olsen, B. R., and Jaenisch, R. (1994) Mice lacking alpha 1 (IX) collagen develop noninflammatory degenerative joint disease. *Proc. Natl. Acad. Sci. USA* **91**, 5070–5074
26. Helminen, H. J., Kiraly, K., Peltari, A., Tammi, M. I., Vandenberg, P., Pereira, R., Dhulipala, R., Khillan, J. S., Ala-Kokko, L., Hume, E. L., Sokolov, B. P., and Prockop, D. J. (1993) An inbred line of transgenic mice expressing an internally deleted gene for type II procollagen (COL2A1). *J. Clin. Invest.* **92**, 582–595
27. Lapvetelainen, T., Hyttinen, M., Lindblom, J., Langsjo, T. K., Sironen, R., Li, S. W., Arita, M., Prockop, D. J., Puustjarvi, K., and Helminen, H. J. (2001) More knee joint osteoarthritis (OA) in mice after inactivation of one allele of type II procollagen gene but less OA after lifelong voluntary wheel running exercise. *Osteoarth. Cartilage* **9**, 152–160
28. Nakata, K., Ono, K., Miyazaki, J., Olsen, B. R., Muragaki, Y., Adachi, E., Yamamura, K., and Kimura, T. (1993) Osteoarthritis associated with mild chondrodysplasia in transgenic mice expressing alpha 1 (IX) collagen chains with a central deletion. *Proc. Natl. Acad. Sci. USA* **90**, 2870–2874
29. Saamanen, A., Salminen, H., Dean, P., Crombrugge, B. d., Vuorio, E., and Metsaranta, M. (2000) Osteoarthritis-like lesions in transgenic mice harboring a small deletion mutation in type II collagen gene. *Osteoarth. Cartilage* **8**, 248–257
30. Seegmiller, R. E., Ryder, V., Jackson, R., Rodriguez, R., Vu, H., Babcock, W., Poole, R., Crowe, R., and Bridgewater, L. (2001) Comparison of two collagen mutant mouse lines that serve as models of early-onset osteoarthritis in human chondrodysplasia. *Osteoarth. Cartilage* **9**, S15

Received for publication November 5, 2001.
Revised for publication January 23, 2002.